Available online at www.sciencedirect.com
ScienceDirect
Developmental Biology 297 (2006) 446–460
DEVELOPMENTAL BIOLOGY
www.elsevier.com/locate/ydbio

Misexpression of acetylcholinesterases in the *C. elegans pha-2* mutant accompanies ultrastructural defects in pharyngeal muscle cells

Catarina Mörck [a], Claes Axäng [a], Mattias Goksör [b], Marc Pilon [c,*]

[a] *Department of Cell and Molecular Biology, Göteborg University, Box 462, SE-405 30 Göteborg, Sweden*
[b] *Department of Physics, Göteborg University, SE-412 96, Göteborg, Sweden*
[c] *Department of Chemical and Biological Engineering, Lundberg Laboratory, Chalmers University, Box 462, SE-405 30, Göteborg, Sweden*

Received for publication 26 October 2005; revised 8 May 2006; accepted 18 May 2006
Available online 24 May 2006

Abstract

pha-2 is the *Caenorhabditis elegans* homolog of the vertebrate homeobox gene *Hex*. Embryonic expression of *pha-2* is mostly pharyngeal and the only described mutant allele of *pha-2* results in a severe pharyngeal defect in which certain muscle cells (pm5 cells) and neurons are grossly deformed. Here, we performed a detailed characterization of the *pha-2* phenotype using cell-type-specific reporters, physical manipulation of the nuclei in pharyngeal muscle cells using "optical tweezers", electron microscopy, staining of the actin cytoskeleton as well as phenotypic rescue and ectopic expression experiments. The main findings of the present study are (i) the *pha-2* (*ad472*) mutation specifically impairs the pharyngeal expression of *pha-2*; (ii) in the *pha-2* mutant, the cytoskeleton of the pm5 cells is measurably weaker than in normal cells and is severely disrupted by large tubular structures and organelles; (iii) the pm5 cells of the *pha-2* mutant fail to express the acetylcholinesterase genes *ace-1* and *ace-2*; (iv) ectopic expression of *pha-2* can induce ectopic expression of *ace-1* and *ace-2*; and (v) the *anc-1* mutant with mislocalized pm5 cell nuclei occasionally shows an isthmus phenotype similar to that of *pha-2* worms.

Keywords: *pha-2*; *anc-1*; *Hex*; *Caenorhabditis elegans*; Acetylcholinesterase; Pharynx

Introduction

The *Caenorhabditis elegans* pharynx is an 80-cell neuromuscular tube located at the anterior end of the worm where it is responsible for the ingestion and maceration of food. There are five cell types present in the pharynx: muscle cells, nerve cells, marginal cells, epithelial cells and gland cells (Albertson and Thomson, 1976). The pharynx is sometimes considered to be evolutionarily related to the heart because (i) like the heart, the pharynx is a rhythmically contracting neuromuscular pump (Avery and Shtonda, 2003); (ii) the muscle cells of the pharynx have autonomous contractile activity reminiscent of cardiac myocytes (Avery and Horvitz, 1989); and (iii) *ceh-22*, the *C. elegans* homolog to the homeobox gene *Nkx2.5* that plays an important role in heart development in vertebrates, participates in pharyngeal development (Haun et al., 1998).

We previously cloned the *pha-2* gene that, when mutated, causes a severe post-embryonic deformation of the pharynx (Mörck et al., 2004). During pharyngeal development, a laminin-covered primordium that is initially spherical elongates unevenly to form a tube with two bulbs, called the posterior bulb and the metacorpus, separated by a narrow passage called the isthmus. Anterior to the metacorpus lies the procorpus, which is also a narrowed part of the organ. We have shown previously that the isthmus separating the muscular bulbs is produced by the anterior elongation of cells that retain their nuclei embedded within the posterior bulb. Hence, the isthmus is itself devoid of nuclei. In *pha-2* embryos, the nuclei of the cells that form the isthmus are positioned within the isthmus as these cells elongate. Following the onset of pharyngeal pumping in the *pha-2* mutant, the isthmus gradually deforms by thickening and shortening, eventually becoming a thick bulge between the two muscular bulbs by the adult stage.

The molecular identity of *pha-2* did not provide a direct explanation for the *pha-2* phenotype: *pha-2* encodes a

* Corresponding author. Fax: +46 31 773 3801.
E-mail address: marc.pilon@chembio.chalmers.se (M. Pilon).

0012-1606/$ - see front matter © 2006 Elsevier Inc. All rights reserved.
doi:10.1016/j.ydbio.2006.05.020

homeodomain protein homologous to the vertebrate *Hex*, a gene with a well-documented role in the development of foregut and of foregut-derived organs such as liver, lung and pancreas (Bogue et al., 2000; Martinez Barbera, 2000; Smithers and Jones, 2002). Here, we present a detailed description of the *pha-2* phenotype, including direct measurements of cytoskeletal strength in the muscle cells of the isthmus using optical tweezers and an ultrastructural analysis. We also show that the isthmus muscle cells fail to express two important acetylcholinesterase (AChE) genes, *ace-1* and *ace-2*, that these genes are ectopically expressed in embryos that ectopically express *pha-2*, and that the *anc-1* mutant, in which pm5 nuclei are occasionally misplaced into the isthmus, shows a rare *pha-2* mutant-like isthmus phenotype. Based on these results, we conclude that the combined failure to sequester the pm5 nuclei in the posterior bulb and to express the *ace-1* and *ace-2* genes in the isthmus may together cause the isthmus deformation in the *pha-2* mutant.

Materials and methods

Nematode strains and culture

Maintenance and handling of worms were as described (Sulston and Hodgkin, 1988). Wild-type parent strain used was the *C. elegans* Bristol variety strain, N2 (Brenner, 1974). The *ace-1*(*ok663*), *ace-2*(*g72*), *ace-1*(*p1000*);*ace-2*(*g72*), *anc-1*(*e1802*) and *pha-2*(*ad472*) mutant worms were provided by the *C. elegans* Genetics Center (Minneapolis, Minnesota). For experiments to test pm5 cell identity, wild-type worms carrying the *pglc-2*:*lacZ* (Laughton et al., 1997) construct were kindly provided by Adrian Wolstenholme. The strain EC668, which contains a translational *ifa-1*::*GFP* fusion introduced by particle bombardment into an *unc-119*(*ed3*) background, was kindly provided by Ekkehard Schulze (Karabinos et al., 2002). For optical tweezer experiments, wild-type N2 and *pha-2* mutant L1 larvae carrying the plasmid *pPHA-2*::*GFP-E* (Mörck et al., 2004) were used. Worms transgenic for *pBK125* (*hsp-16-2*:*gfp*; from Andrew Fire) were used as controls for some ectopic expression experiments. Worms transgenic for *myo-2*::*GFP* or the *pha-2* translational reporter *pPHA-2*::*GFP-A* were also used as controls in some experiments (Mörck et al., 2004). Worms were cultured at 20°C unless otherwise noted.

cDNA isolation and sequencing

Total RNA was isolated from wild-type worms grown on NGM plates using a guanidium isothiocyanate-based protocol (Krause, 1995). First-strand cDNA synthesis was performed using the kit 5′RACE System for Rapid Amplification of cDNA ends (Invitrogen) with a *pha-2*-specific primer, pha-2(+318): 5′-CTCAAAGACTTTGCAAGTTTCTTC-3′. *pha-2* cDNA was then amplified by a polymerase chain reaction (PCR) using Taq polymerase (Roche) and a nested primer, pha-2(+297): 5′-CGCTCTTGGGGACTCAAATAC-3′ or pha-2(+258): 5′-TGCTCCAACGCATCGGTTTGC-3′, together with one of the following primers: pha-2(−398): 5′-CCACGAAGACATACGATACC-3′, pha-2(−332): 5′-ATGCTCTTCCTCTCACTCTTAGC-3′ or pha-2(−42): 5′-CCAATACCTACAGGCAGCGAA-3′. The PCR products were separated by agarose gel electrophoresis then purified using a Qiaquick Gel Extraction Kit (Qiagen) and subcloned into the pGEM T-easy vector using the pGEM T-easy Vector Kit (Promega). Plasmids harboring the PCR fragments were sequenced by MWG Biotech (Germany).

Construction of reporter plasmids

Unless otherwise noted, DNA from single worms were used as template to amplify DNA regions of interest. Worms were lysed in SWLB buffer containing proteinase K (50 mM KCl, 2.5 mM $MgCl_2$, 10 mM Tris, pH 8.3, 0.45% Nonidet P-40, 0.45% Tween-20, 0.01% gelatin and 100 μg/ml Proteinase K). PCR was performed with platinum Pfx polymerase (Invitrogen) or *PfuUltra* (Stratagene) together with the supplied reaction buffers. The PCR products were separated by agarose gel electrophoresis then purified using a Qiaquick Gel Extraction Kit (Qiagen). The PCR fragments were A-tailed with Taq polymerase (Roche) and subcloned into the pGEM T-easy vector (Promega).

pPHA-2FRAMESHIFT::*GFP*. A 2.7 kb 5′-UTR sequence from the *pha-2* gene was PCR amplified using the following primers: M6.3PL: 5′-GACCTGCAGGAATTCCGATTATCATGGGCTG-3′ (PstI site underlined) and pet031127a: 5′-GCTCTAGATGGTAATGTGAAGAACGGAGC-3′ (XbaI site underlined) creating fragment 1. A 3.2-kb sequence containing the whole *pha-2* gene was amplified with the following primers pet031127b: 5′-GCTCTAGAGCCTTTTCAATTAGCCTCATCTC-3′ (XbaI site underlined) and M6.3PRXbaI: 5′-CTCTAGAACCATGAGACAGAAACGG-3′ (XbaI site underlined), creating fragment 2. The gel-purified products were A-tailed with Taq polymerase (Roche) and subcloned into the *pGEM T-easy* vector (Promega). Fragment 1 was inserted as a PstI-XbaI fragment into the corresponding sites of *pPD95.69* (a kind gift from Andrew Fire) creating *pPHA-2_fragment1*. Fragment 2 was inserted as a XbaI-XbaI fragment into the XbaI site of *pPHA-2_fragment1* to create *pPHA-2FRAMESHIFT*::*GFP*, with 7 nucleotides (5′-ATCTAGA-3′) introduced downstream of the predicted start ATG (see Fig. 1). A 700-bp region of *pPHA-2FRAMESHIFT*::*GFP* centered around the inserted frameshift was sequenced to confirm that the desired nucleotide changes were correctly made.

pPHA-2_ad472::*GFP*. A 1.5-kb genomic DNA sequence covering *the pha-2* (*ad472*) point mutation was PCR amplified using the following primers: pha-2_1018 nt: 5′-CACAGGTGAACTGTCTCTAATCC-3′ and M6.3_ex1-3_3: 5′-GGCTCAATTCGTTGATTCAG-3′. Single *pha-2* mutants were used as template. The gel-purified PCR product was inserted as a 1.4-kb BssHII-SexAI fragment into the corresponding sites of *pPHA-2*::*GFP-A* (Mörck et al., 2004), thus creating *pPHA-2_ad472*::*GFP*. The plasmid was ethanol precipitated with ammonium acetate and sent for sequencing to MWG Biotech (Germany) to confirm the structure.

pHSP::*PHA-2cDNA*. The full-length *pha-2* cDNA was PCR amplified using as template the plasmid *pGEM-Teasy-PHA2cDNA* (Mörck et al., 2004) and the following primers: pha-2_cDNA_forward: 5′-GCTAGCATGGAACCAAATAAAAAAATG-3′ (NheI site underlined) and pha-2_cDNA_reverse: 5′-GCTAGCTTAACCATGAGACAGAAACGG-3′ (NheI site underlined). The product was inserted as a NheI-NheI fragment into the NheI site of *pPD49.83* (a kind gift from Andrew Fire).

pHSP::*PHA-2cDNA*::*GFP*. The full-length *pha-2* cDNA was amplified from *pGEM-Teasy-PHA2cDNA* using the primers PHA2cDNA-1: 5′-ACTGCAGAAAGATGGAACCAAATAAAAAAATGTTT-3′ (PstI site underlined) and PHA2cDNA-2: 5′-CTCTAGAACCATGAGACAGAAACGGATTAGACGA-3′ (XbaI site underlined), then subcloned as a PstI-XbaI fragment into the corresponding sites of *pPD95.69* to create *pPD95.69*::*PHA-2cDNA*::*GFP*. This construct was then used as a template for a PCR reaction using the primers cPHA2GFP-1: 5′-*GCTAGC*ATGGAACCAAATAAAAAAATG-3′ (NheI underlined) and cPHA2GFP-2: 5′-*GCTAGC*CTATTTGTATAGTTCATCCATG-3′ (NheI underlined) to amplify a fragment containing the PHA2 cDNA fused in frame at its 3′ end with the NLS-tagged GFP gene. This was cleaved with NheI and subcloned into the corresponding site of the *pPD49.78* plasmid to create *pHSP*::*PHA2cDNA*::*GFP*. In this later construct, the PHA-2::GFP fusion gene is regulated by the hsp16-2 promoter.

pACE-1::*GFP*. 4 kb of 5′-UTR sequence as well as the first four codons of *ace-1* were PCR amplified using the following primers: ace-1_forward: 5′-CTGCAGCCATTCCTCAACCTTCTTAC-3′ (PstI site underlined) and ace-1_reverse: 5′-GTCGACGGAATTTCGCATGCTTCTTC-3′ (SalI site underlined). The gel-purified product was A-tailed with Taq polymerase (Roche) and subcloned into the *pGEM T-easy* vector (Promega) and further inserted as a PstI-SalI fragment into the corresponding sites of *pPD95.69* (a kind gift from Andrew Fire).

pACE-2::*GFP*. 3.7 kb of 5′-UTR sequence and the first three codons were PCR amplified with the following primers: ace-2_forward: 5′-GGATCCCCCTCTCCGTCTCGTACTTC-3′ (BamHI site underlined) and ace-2_reverse: 5′-GGATCCCGCTCGCATGACCTGAGAGTG-3′ (BamHI site underlined). The gel-purified PCR product was A-tailed with TAQ polymerase (Roche) and subcloned into *pGEM T-easy* vector (Promega) and inserted as a BamHI-BamHI fragment into the BamHI site of *pPD95.69*.

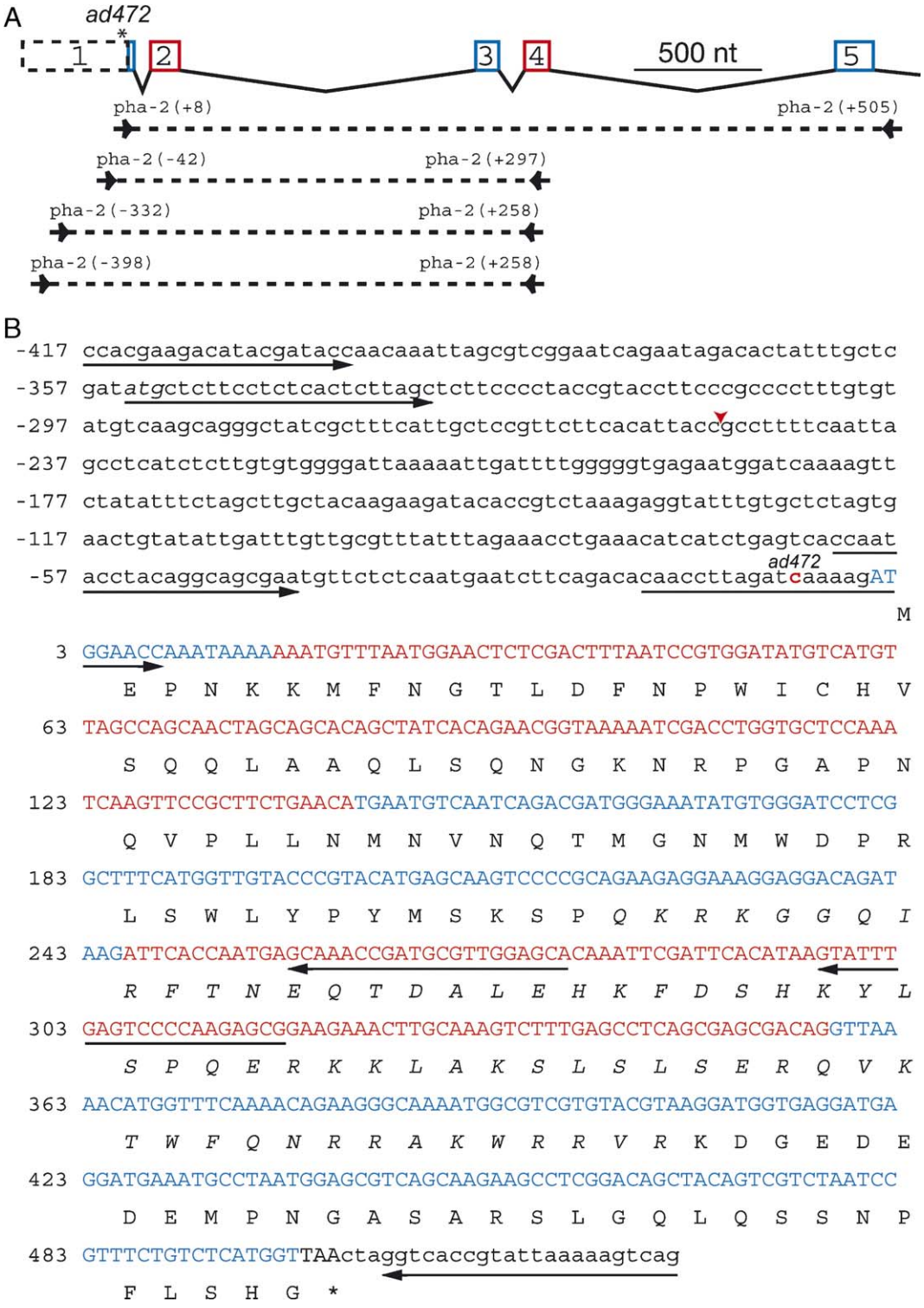

Fig. 1. Revised *pha-2* gene structure. Panel A shows the revised structure for the *pha-2* gene. Dashed box indicates 5′UTR, boxes indicate translated exons. The relative positions of the primers that gave RT-PCR products that are also shown. These products consisted of clean single bands that were sequenced and found to be consistent with the gene structure presented. Panel B shows the sequence of the *pha-2* cDNA and the corresponding translated frame. Sequences corresponding to the primers used in the RT-PCR reactions are underlined with arrows (see Materials and methods). The formerly predicted start ATG is italicized at the beginning of the pha-2(−332) primer. The cytosine that is mutated to a thymidine in the *pha-2*(*ad472*) allele is indicated in red bold, 6 positions upstream from the experimentally validated start ATG. The *pha-2* open reading frame is shown in capital letters, and exons are shown in alternating blue and red colors, with the translated frame expressed using the one-letter amino acid code shown just below. The amino acids that are part of the homeodomain are italicized. Position 1 is here assigned to the "A" in the confirmed start ATG and corresponds to genomic position 636,687 of the *C. elegans* chromosome X (according to the WormBase web site, http://www.wormbase.org, release WS153). The red arrowhead at position −250 indicates the site of insertion of the nucleotides 5′-ATCTAGA-3′ in the construct *pPHA-2FRAMESHIFT*::*GFP*.

pACE-4;ACE-3::*GFP*. 4.0 kb of 5′-UTR sequence and the first three codons of the *ace-4* gene were PCR amplified with the following primers: ace-4;ace-3_forward: 5′-GGATCCGTCTTCGTCTTAGGTTTAGGC-3′ (BamHI site underlined) and ace-4;ace-3_reverse: 5′-GGATCCTGGTTTCATCGGC-GATCCGAG-3′ (BamHI site underlined). The gel-purified PCR product was treated exactly as the product produced in the *pACE-2*::*GFP* reaction described above.

Generation of transgenic worms

Transformation was performed using established methods (Mello and Fire, 1995) by microinjecting the distal ovary ends of hermaphrodites with a mix of the plasmids pRF4, pBluescript (Stratagene) and test DNA. pRF4 was used as a transformation marker: this plasmid carries a mutant form of a collagen gene that causes a roller (Rol) phenotype in transgenic animals (Mello and Fire, 1995). All plasmids were purified with a Qiagen Miniprep Kit (Qiagen) and used at concentrations of 10 to 50 ng/μl. Transgenic worms were identified by the Rol phenotype.

lacZ staining

Wild-type and *pha-2* worms carrying the extrachromosomal array *pglc-2*:*lacZ* were stained for β-galactosidase activity using slight modifications of previously published methods (Fire, 1992). Briefly, worms from one culture plate were recovered and washed three times with M9 buffer (22 mM KH_2PO4, 22 mM Na_2HPO_4, 85 mM NaCl, 1 mM $MgSO_4$) then transferred to a 0.5 ml reaction tube in which they were sedimented by gentle centrifugation before removing all excess liquid. The samples were snap frozen by floating the tubes in liquid nitrogen. The worms were then dried under vacuum while being centrifuged for 45 min. The worms were fixed for 3 min with 250 μl of ice-cold acetone then again dried under vacuum until all acetone had evaporated. 250 μl of staining solution (for 1 ml: 200 μl Na_2PO_4 buffer (1 M pH 7.5), 1 μl MgCl2 (1 M), 0.4 μl SDS (10%), 100 μl redox buffer (100 mM potassium ferricyanide +100 mM potassium ferrocyanide), 1.5 μl kanamycine (50 mg/ml), 2 μl DAPI (1 mg/ml), 2 μl X-gal (20%) and 693.1 μl dH_2O) was added to the tubes and the worms were stained overnight on a shaking table. The worms were washed twice with PBS and mounted on agarose pads (2% in M9) for observation.

Phalloidin staining

Wild-type and *pha-2* adult worms were picked to 1.5-ml reaction tubes containing S basal buffer (145 mM NaCl, 50 mM KPO_4, 10 μg/ml cholesterol), sedimented by gentle centrifugation for 1 min then washed three times with S basal. Excess liquid was removed, and the samples were snap frozen by floating the tubes in liquid nitrogen. The worms were then dried under vacuum while being centrifuged for 45 min. Approximately 100 μl of ice-cold acetone was added to the dried worm pellet and removed immediately. The worms were again vacuum dried until all acetone was gone. 50 μl of "S mix" containing phalloidin–FITC were added (250 μl Na_2PO_4 (0.8 M, pH 7.5), 1 μl $MgCl_2$ (1 M), 4 μl SDS (1%), 1 μl phalloidin–FITC) and the worms were stained for 40 min. Worms were washed twice with PBBT buffer (PBS + 0.5% BSA + 0.5% Tween-20). 20 μl mounting solution (0.01 g phenylendiamin, 100 μl PBS, 900 μl H_2O) was added to each tube and the worms were studied by confocal microscopy.

Optical tweezers

Wild-type and *pha-2* mutants carrying an extrachromosomal *pPHA-2*::*GFP-E* construct (Mörck et al., 2004) were mounted on 2% agarose pads (in M9 buffer) and paralyzed with one droplet of levamisole (100 mM). The pm5 nuclei were localized via their expression of GFP and trapped by optical tweezers (Goksör et al., 2004; Simmons et al., 1996). The optical trap in the sample was formed by focusing over 4 W of the laser light from a continuous Nd:YVO4 laser operating at 1064 nm by using the microscope objective. The stage was then moved by set distances using electrical motors. The ability of the optical tweezers to maintain the pm5 nucleus within the optical trap was then determined. For each tested pm5 nucleus, the data were expressed in terms of micrometers of movement allowed before the nucleus escaped the trap. The exact optical force applied to the pm5 nucleus was not determined due to the non-homogeneous interior of *C. elegans*. However, we estimate the optical force applied to be well over 500 pN. The samples were continuously monitored using a Hamamatsu video camera connected to a Nikon microscope.

Ectopic expression experiments

For this study the following constructs were introduced into wild-type worms: *pHSP*::*PHA-2cDNA* + *pACE-1*::*GFP*, or *pHSP*::*PHA-2cDNA* + *pACE-2*::*GFP*, or *pHSP*::*PHA-2cDNA* + *pACE-4;ACE-3*::*GFP*, or *pHSP*::*PHA-2cDNA*::*GFP*, or *pBK125*. Young transgenic adult hermaphrodites were allowed to lay eggs for 1 h at 20°C. All adults were removed, and the eggs were heat shocked for 1 h at 33°C then transferred to 15°C. Embryos were scored over 6–14 h after the heat shock.

Aldicarb tests

Day 1: aldicarb (105 mM in 70% ethanol; ChemService (West Chester, PA)) was added to autoclaved and cooled NGM media to produce plates with different concentration of aldicarb: 0 mM, 0.2 mM, 0.6 mM, 0.8 mM, 1.6 mM or 2.0 mM. Day 2: OP50 bacteria were spread onto the plates. Day 3: Wild-type or *anc-1* mutant embryos carrying the extrachromosomal array *pPHA-2*::*GFP-E* (Mörck et al., 2004) were transferred to the aldicarb plates. Day 4: movement, feeding ability and pharynx morphology were scored.

DIC and epifluorescence microscopy

Worms were mounted on 2% agarose pads (in M9 buffer), paralyzed by one drop of levamisole (100 mM) and examined with a Zeiss Axioplan compound microscope using Nomarski optics or an FITC filter to visualize GFP. Digital images were acquired using an attached AxioCam digital camera.

Confocal microscopy

Worms were mounted on dried 2% agarose pads (in H_2O), paralyzed by one drop of levamisole (100 mM) and examined by a Zeiss LSM 510 META System connected to an inverted Zeiss Axiovert 200 microscope.

Electron microscopy

Live nematodes intended for transmission electron microscopy (TEM) were cut under the dissection microscope immediately behind the pharyngeal region in order to facilitate penetration of fixative solutions to the anatomical region of interest. The anterior portions of the animals were immersed overnight in a mixture of 2% paraformaldehyde, 2.5% glutaraldehyde, and 0.01% sodium azide in 0.05 M sodium cacodylate buffer, pH 7.2, at 4°C. After rinsing in cacodylate, specimens were postfixed 2 h in 1% OsO4 with addition of 1% potassium ferrocyanide at 4°C, rinsed in distilled water, and stained en bloc with 0.5% uranyl acetate for 1 h in room temperature in the dark. Dehydration in a graded series of ethanol was followed by substitution with propylene oxide and epoxy resin (Agar 100, Agar Scientific, UK). Plastic infiltrated specimens were properly oriented in flat moulds to allow transverse sectioning from the cut surface of the animal before curing by heat. Sectioning was performed with a Reichert Ultracut E ultramicrotome (Leitz Co., Vienna, Austria) fitted with diamond knives. First semithin (1 μm) sections were collected and stained with Richardson's stain to identify the pharyngeal regions of interest by light microscopy which was then subjected to ultramicrotomy at a thickness setting of 60 nm. Sections were collected on copper grids, contrasted with uranyl acetate and lead citrate and examined in a LEO 912AB Omega TEM (Carl Zeiss NTS, Oberkochen, Germany). Digital images were captured with a MegaView III camera (Soft Imaging Systems, Münster, Germany).

Results

Revision of the pha-2 gene structure

In our previous study of the *pha-2* gene, we were not able to confirm the correctness of the start ATG in the *pha-2* gene structure predicted by WormBase (WormBase web site: http://www.wormbase.org) (Mörck et al., 2004). No *pha-2* cDNA has been recovered from cDNA libraries, and our own efforts at verifying the gene structure using 5′ RACE or RNAse protection assays have been unsuccessful (data not shown). In a further effort to confirm the start

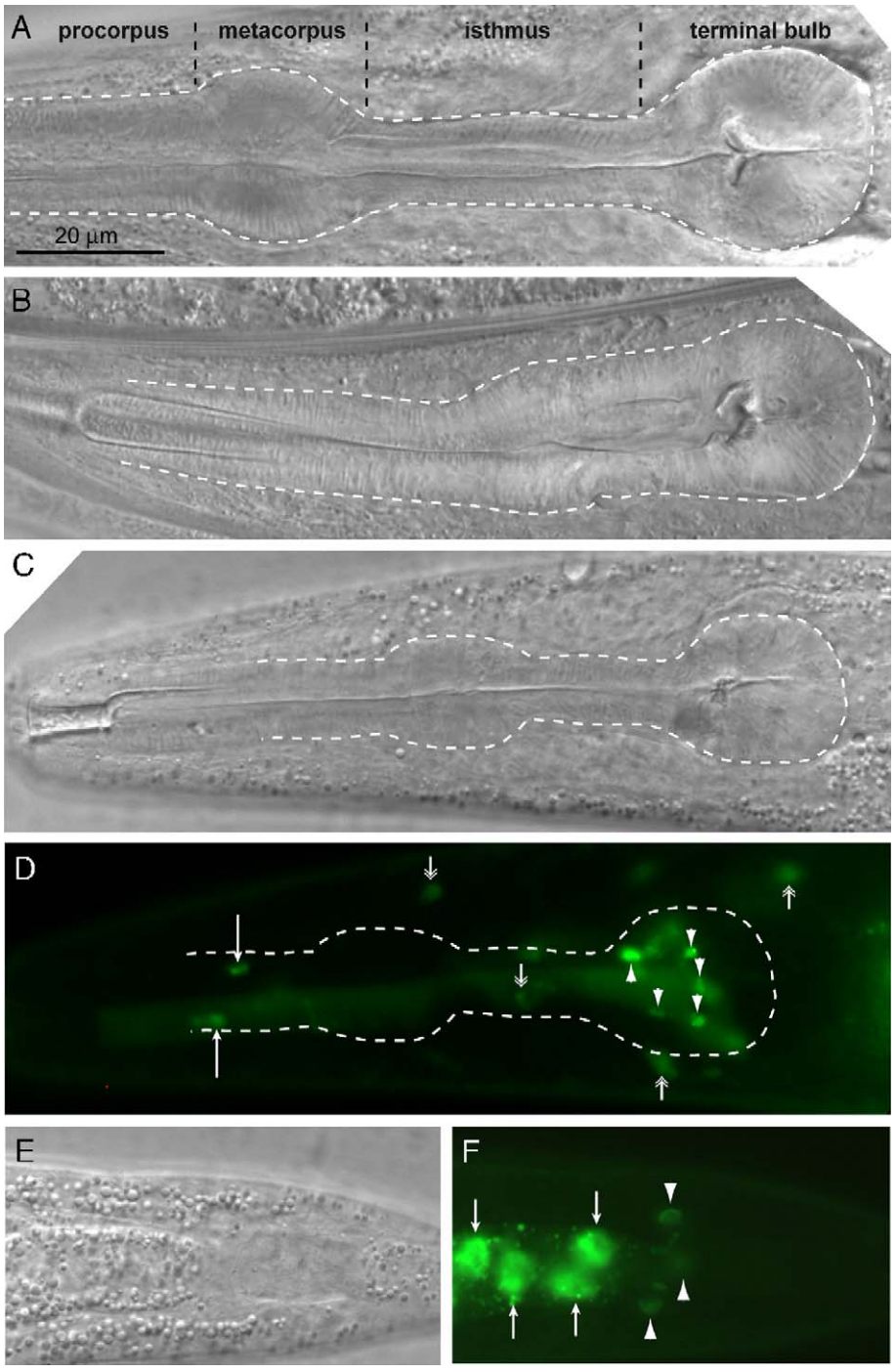

Fig. 2. Rescuing activity and expression profile of mutated *pha-2*. Panels A and B show DIC images of wild-type and *pha-2* mutant pharynxes, respectively. Panel C shows a *pha-2* mutant worm at the L4 stage transgenic for the *pPHA-2FRAMESHIFT*: :*GFP*, and panel D shows the GFP profile from the same specimen as in panel C. Note that the *pPHA-2FRAMESHIFT*: :*GFP* is fully capable of rescuing the *pha-2* mutant phenotype (note the narrow isthmus in panel D) and of supporting expression in the pm5 cell nuclei (indicated by arrowheads in panel D). Also in panel D, arrows point at epithelial cells in the procorpus and double arrows indicate extrapharyngeal neurons. Panels E and F show DIC and corresponding GFP images of the posterior part of the same worm, revealing GFP-positive intestinal (arrows) and rectal cells (arrowheads).

ATG, we designed several primers corresponding to positions upstream of the predicted start at approximately 100-bp intervals and also one located in the first predicted intron. These primers were used in RT-PCR reactions together with primers from within exon sequences that we previously confirmed is part of the cDNA (Mörck et al., 2004). The primer pha-2(−398) that anneals 63 nt upstream of the original predicted start, the primer pha-2(−332) that anneals at the original predicted start, and the primer pha-2 (−42) that anneals within the original predicted first intron each gave a single RT-PCR product together with the pha-2 (+297) or pha-2(+258) primers. Primers annealing upstream of position −417 gave no product. Based on the sequencing of the RT-PCR products, we revised the *pha-2* gene structure in two important ways: (i) the start ATG is now located 219 nucleotides upstream of the glutamine that marks the beginning of the highly conserved homeodomain; and (ii) what was formerly considered to be the first intron is actually part of the 5′-UTR sequence. The revised structure is summarized in Fig. 1.

The revised *pha-2* gene structure predicts that the nucleotide triplet initially proposed to act as a start codon is actually located far upstream (−177 nt) of the actual start ATG. To further test this, a full-length PHA-2: :GFP translational fusion carrying 2.7 kb of *pha-2* 5′UTR was made in which we disrupted the open reading frame of the original predicted start codon with a 7 nucleotide insertion.

Table 1
Expression profile of the control construct *pPHA-2*: :*GFP-A* (Mörck et al., 2004) compared to *pPHA-2_ad472*:*GFP*, which contains the *pha-2*(*ad472*) point mutation

Expression	pPHA-2: :GFP-A (n = 66) (%)	pPHA-2_ad472:GFP (n = 50) (%)
Extrapharyngeal neurons	98	100
Epithelial cells in pharynx	89	67
pm4 (metacorpus muscle cells)	44	6
pm5 (isthmus muscle cells)	76	0
I4 (pharyngeal interneuron)	87	0
Intestinal cells	79	65
Rectal cells	89	49

Adult worms were scored for the presence of GFP expression in the indicated cell type.

The inserted nucleotides cause a frameshift ending in a STOP codon 45 bases downstream of the inserted nucleotides (see Fig. 1). This construct supported GFP expression in the pharyngeal epithelial cells, pm4 and pm5 cells, in extrapharyngeal neurons, intestinal and rectal cells and, importantly, was also equally competent as a wild-type control at rescuing the *pha-2* phenotype, with well over 50% of the transgenic worms showing moderate to excellent rescue of the isthmus defect (Fig. 2). This experiment demonstrates beyond doubt that the correct start ATG must be located downstream from the original prediction.

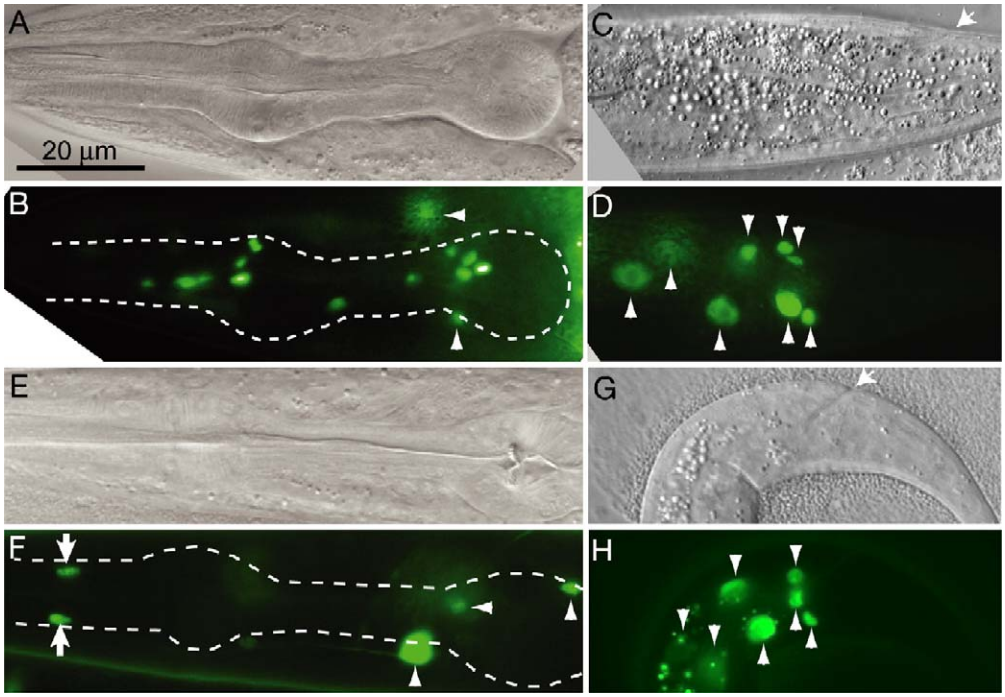

Fig. 3. The *ad472* mutation affects only pharyngeal expression of *pha-2*. DIC and corresponding GFP images of the pharynx and tail of L2 or L3 larvae transgenic for the wild-type control translational reporter *pPHA-2*: :*GFP-A* (A–D) or the mutated construct *pPHA-2_ad472*:*GFP* (E–H). The pharynx is outlined with dashed lines in panels B and F, and the anus is indicated with an arrow in panels C and G. The mutant reporter is expressed in pharyngeal epithelial cells (arrows in panel F) and cells outside the pharynx (arrowheads in panel F show extrapharyngeal neurons; arrowheads in panel H show rectal and/or intestinal cells) but shows no expression in the pm5 cells or metacorpus (some cells indicated with arrowheads within the dashed line in panel F are extrapharyngeal neurons above or below the focal plane and lying outside the pharynx). In contrast, the control construct shows strong expression in several pharyngeal cells within the metacorpus and posterior bulb (within the dashed lines in panel B), as well as in extrapharyngeal neurons (arrowheads in panel B) and rectal and/or intestinal cells (arrowheads in panel D).

The ad472 mutation affects only pharyngeal expression of pha-2 in the pharynx

The revised *pha-2* gene structure has serious implications for the only known mutant *pha-2* allele, i.e., *ad472*, because it now places that point mutation 6 nucleotides upstream of the start codon, rather than at amino acid position 58, as was previously thought (Mörck et al., 2004). To evaluate the impact of the *ad472* mutation on the expression of the *pha-2* gene, we constructed a full-length PHA-2::GFP translational fusion carrying 2.7 kb of *pha-2* 5′UTR in which the same point mutation as in the *ad472* allele was introduced. As previously reported, introduction of a control PHA-2::GFP translational fusion construct (*pPHA2::GFP-A*) often causes some pharyngeal deformation and shows pharyngeal GFP expression in the pm5 cells, cells in the metacorpus, and pharyngeal epithelial cells, as well as in many extrapharyngeal neurons, intestinal cells and rectal cells (Mörck et al., 2004). Remarkably, animals from several independent transgenic lines carrying the construct with the *ad472* mutation (*pPHA2_ad472::GFP*) exhibited no expression in the pm5 cells and I4 interneuron and significantly decreased levels in the metacorpus but had pharyngeal epithelial and extrapharyngeal expression profiles not readily distinguishable from the wild-type construct in this assay (Table 1, Fig. 3). Note that the minor frequency deviations shown in Table 1 likely reflect differences in the properties of the various extrachromosomal arrays. However, our main finding, i.e., that *pPHA2_ad472::GFP* is not expressed in the pm5 and I4 cells, holds true in many independent lines. It is therefore possible that *pha-2* plays important roles outside of the pharynx, but that only pharyngeal functions are impaired in the *ad472* allele.

The *pPHA-2_ad472::GFP* construct showed no rescuing activity when introduced into a *pha-2* mutant background: none of the transgenic worms showed any improvement in the isthmus phenotype. This result indicates that expression of the *pha-2* gene in the pm5 and/or I4 cells is necessary to rescue the *pha-2*(*ad472*) isthmus phenotype and also serves as a control against the possibility that the rescuing ability of the frame-shifted construct discussed in the previous section could result from the overexpression of a truncated protein from the high copy number transgene arrays.

The pm5 cell nuclei have not (fully) adopted a pm4 identity

The pharynxes in *pha-2* mutants are severely deformed with a short and thickened isthmus (Fig. 2B). We have previously hypothesized that the pm5 muscle cells forming the isthmus have a mistaken identity and acquired a pm4-like

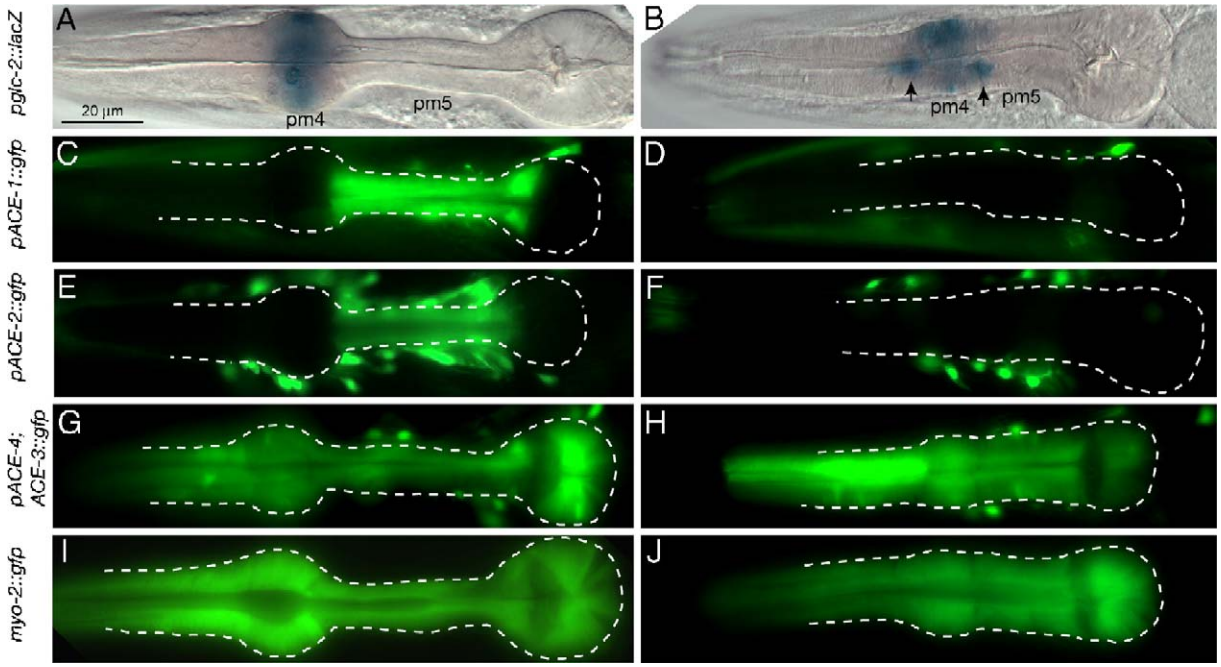

Fig. 4. The acetylcholinesterase *ace-1* and *ace-2* genes are not expressed in the isthmus of *pha-2* mutant worms. Wild-type (A) or *pha-2* mutant (B) worms transgenic for a *pglc-2::lacZ* reporter were stained to visualize the localization of lacZ. The general positions of the pm4 and pm5 cells are indicated. Note that in wild-type, expression of *glc-2::lacZ* is restricted to the pm4 cells and that these are well confined within the metacorpus. In the *pha-2* mutant, the pm4 nuclei are more scattered within the metacorpus and some seem to be localized slightly into the procorpus and isthmus (indicated by arrows). The pm5 nuclei are negative for lacZ in both genotypes (they would be localized quite centrally within the mutant isthmus). Panels C and D show the expression of a *pACE-1::GFP* reporter in wild-type and *pha-2* worms, respectively. Note that the mutant expresses no *pACE-1::GFP* in the isthmus, but supports extrapharyngeal expression. Panels E and F show the expression of a *pACE-2::GFP* reporter in wild-type and *pha-2* worms, respectively. Note that the mutant expresses no *pACE-2::GFP* in the isthmus, but supports extrapharyngeal expression. Panels G and H show expression of a *pACE-4;ACE-3::GFP* reporter. No differences are detectable between wild-type and *pha-2* mutants. Note that both express the reporter in the pm5 cells. Panels I and J shows expression of a *myo-2::GFP* reporter construct expressed in all pharyngeal muscle cells. No difference between wild-type or *pha-2* mutant is seen in the expression profile. Pharynxes are outlined with dotted lines. All worms shown are adults.

cell fate in the *pha-2* mutant (Mörck et al., 2004). Two evidences previously supported this notion: (i) the pm4 cells form the bulk of the metacorpus and are therefore thicker and shorter than wild-type pm5 cells but, perhaps, could be considered as somewhat similar in shape to the pm5 cells of the *pha-2* mutant; (ii) like pm4 cells, the pm5 cells of *pha-2* mutants sustained expression of a CEH-22::GFP reporter well into the adult stage (Mörck et al., 2004). The *glc-2* gene is a marker for pm4 cell identity (Laughton et al., 1997), and we tested whether it was expressed by the pm5 cells of *pha-2* mutants. We found that this is not the case: the reporter was expressed only in the pm4 cells of the mutant animals, just as in wild-type controls (Figs. 4A–B). This indicates that in the mutant, the pm5 cells do not transform to a pm4 cell fate, or at least do not fully transform. A simple identity switch is therefore not an explanation for the *pha-2* phenotype.

The acetylcholinesterase genes ace-1 and ace-2 are not expressed in the pm5 cells of pha-2 mutants

The specific loss of expression of *pha-2* in the pm5 cells of *pha-2*(*ad472*) mutants prompted us to examine the expression of other pm5 markers. The acetylcholinesterase (AChEs) genes *ace-1* and *ace-2* are known to be expressed in many extrapharyngeal cells but, within the pharynx, only in the pm5 muscle cell (Combes et al., 2003; Culetto et al., 1999). We made two translational GFP constructs, *pACE-1::GFP* and *pACE-2::GFP* that were separately injected into wild-type worms to produce several transgenic lines. These expressed GFP in the pattern expected for *ace-1* and for *ace-2* (Figs. 4C, E). By crossing such transgenic worms with *pha-2* mutants, we introduced the transgenes into the *pha-2* genetic background and found that, remarkably, the pm5 cells of *pha-2* worms did not express *pACE-1::GFP* and *pACE-2::GFP*, although expression in other cells was unaffected (Figs. 4D, F).

There are four acetylcholinesterase genes in *C. elegans*. Since expression of *ace-1* and *ace-2* was lost in the mutant, we wished to examine the expression of the two remaining genes, *ace-3* and *ace-4*. These genes are transcribed together from an operon (Combes et al., 2003), and we therefore made one translational GFP reporter construct for the *ace-4; ace-3* genes, *pACE-4;ACE-3::GFP* that we introduced in wild-type and *pha-2* mutant worms. No difference in the expression of *pACE-4;ACE-3::GFP* was found between wild-type and *pha-2* mutants: the construct was expressed in many cells outside the pharynx, including body wall muscle and neurons, and in several muscle cells within the pharynx, including pm3, pm4, pm5 and pm7 (Figs. 4G–H). Thus *ace-4; ace-3* expression is not dependent on *pha-2*. This result also shows that the failure to express *pACE-1::GFP or pACE-2::GFP* in the isthmus cells in *pha-2* mutant is not due to some general "sickness" of these cells, a conclusion also supported by the ability of these cells to express the pharyngeal muscle marker *pmyo-2::GFP* (Figs. 4I–J).

Cytoskeletal defects in the pharynx of pha-2 mutants

We used two direct approaches to better understand the defects within the pm5 cells of *pha-2* mutants: (i) visualization of the actin cytoskeleton using fluorescent-labeled phalloidin and of intermediate filaments using an *ifa-1::GFP* reporter and (ii) electron microscopy. Staining of the actin cytoskeleton using phalloidin showed that actin fibers are present in the mutant pm5 cells and are generally aligned radially and with the same spacing as in wild-type. However, compared to wild-type animals, the actin network is irregular and severely interrupted by gaps of which the

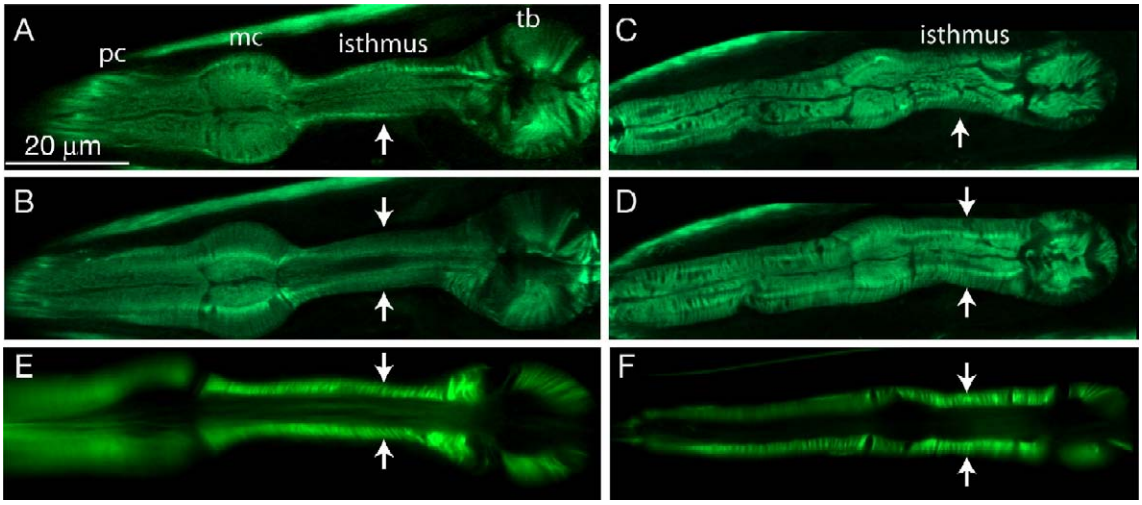

Fig. 5. Visualization of the actin and intermediate filaments cytoskeleton in wild-type and *pha-2* mutants. Adult wild-type (A–B) or *pha-2* mutant (C–D) worms were stained with FITC-labeled phalloidin and observed by confocal microscopy. Two optical sections of the same worms are shown for each genotype. The procorpus (pc), metacorpus (mc), isthmus and terminal bulb (tb) are indicated above these structures in panel A. Arrows indicate the isthmus in all panels. Note that the spacing and alignment of the actin filaments is roughly similar in all figures, but that these are extensively interrupted throughout the mutant pharynx, especially in the isthmus. Panels E and F are confocal planes showing the expression of the GFP fusion reporter for the intermediate filaments A1 in wild-type or *pha-2* mutant isthmuses, respectively. Note that spacing and distribution of the filaments is similar in both genotypes.

identity could not be ascertained by light microscopy (Figs. 5A–D). Intermediate filaments A1, which are expressed by the marginal cells located between the pharyngeal muscle cells (Karabinos et al., 2002), displayed no visible abnormalities in their orientation and spacing (Figs. 5E and F).

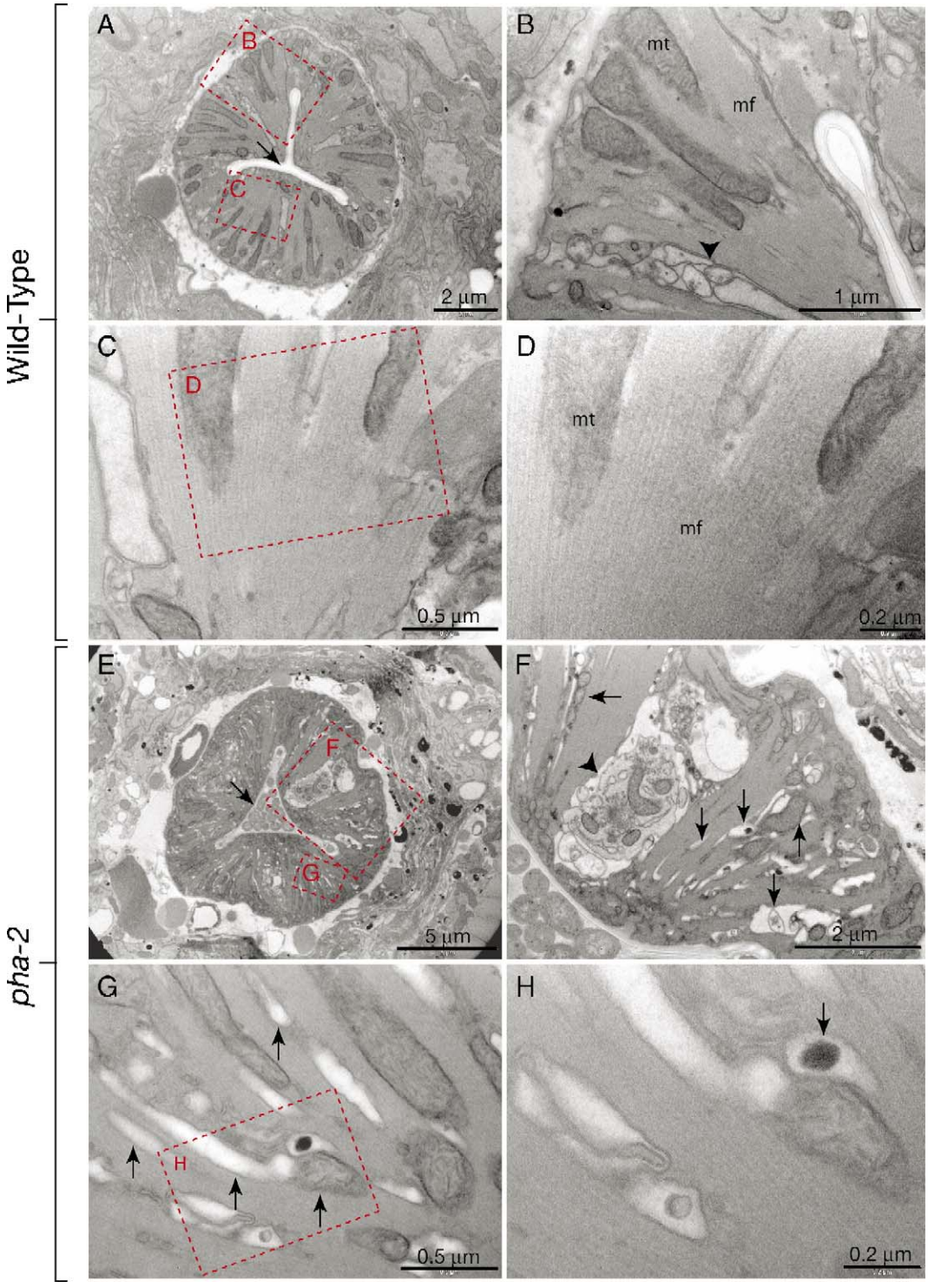

Fig. 6. Ulstrastructural defects in the *pha-2* mutant pm5 pharyngeal cells. Transmission electron micrographs of wild-type (A–D) and *pha-2* mutant (E–H) worms at the level of the isthmus. The dotted frames indicate regions that are magnified in the indicated panels. Mitochondria (mt) and muscle fibers (mf) are labelled in panels B and D). Note that the isthmus lumen is empty in wild type (indicated by an arrow in panel A) but filled with bacteria in the mutant (indicated by an arrow in panel E), indicating that it was contracted at the time of fixation. Note also the presence of organelles and membrane-bound tubulovesicular structures (some are indicated by arrows in panels F and G) within the *pha-2* mutant muscle cells (compare panel A with panel E, and panel D with panel H). Some of the tubulovesicular structures contained electron-dense material (indicated by an arrow in panel H). The muscle cell fold contains small axons seen in cross section in wild type (indicated by an arrowhead in B) but is filled with large organelles in the mutant (arrowhead in panel F).

Electron microscopy revealed that the pm5 cells of *pha-2* mutants are filled with numerous membrane bound electron-transparent tubular compartments that effectively disrupt the tight ordered alignment of the muscle fibers (Fig. 6). Electron-dense granules were also often found within the membrane-bound compartments, suggesting the aggregation of electron-dense molecules, such as proteins or Ca^{2+} ions. Also, a great number of organelles, including many mitochondria, were observed in apparent random distributions within the pm5 cells of mutant animals (Figs. 6E, G). In wild-type worms, in contrast, mitochondria are well ordered and display a somewhat radial, regularly spaced symmetry along the circumference of the isthmus (Fig. 6A). Another interesting observation was that the isthmus of *pha-2* mutants was typically filled with bacteria, suggesting that the isthmus pm5 muscle cells are usually in the contracted state in the mutant (compare Figs. 2B and 6A).

The pm5 cell nuclei can be moved with optical tweezers

One of the more remarkable features of the *pha-2* (*ad472*) mutant phenotype is the presence of several nuclei within the isthmus, a phenotype that is present even before the isthmus becomes severely deformed (Mörck et al., 2004). Could the disruption of the muscle fibers seen at the ultrastructural level (Fig. 6) account for a weakening of the pm5 cell's cytoskeleton that would allow organelles, such as the pm5 nuclei, to move more freely into the isthmus? We directly tested this hypothesis by determining the ease with which the nuclei of the pm5 muscle cells, which make up most of the isthmus volume, could be moved using optical tweezers. Our results show that with the same optical tweezer strength, the pm5 nuclei of *pha-2* mutants could be moved more than three times as much as those of wild-type animals (>3 μm for *pha-2* (*ad472*) vs. <1 μm for wild type; Fig. 7). This is consistent with the hypothesis that the pm5 nuclei are not adequately sequestered in the *pha-2* mutant.

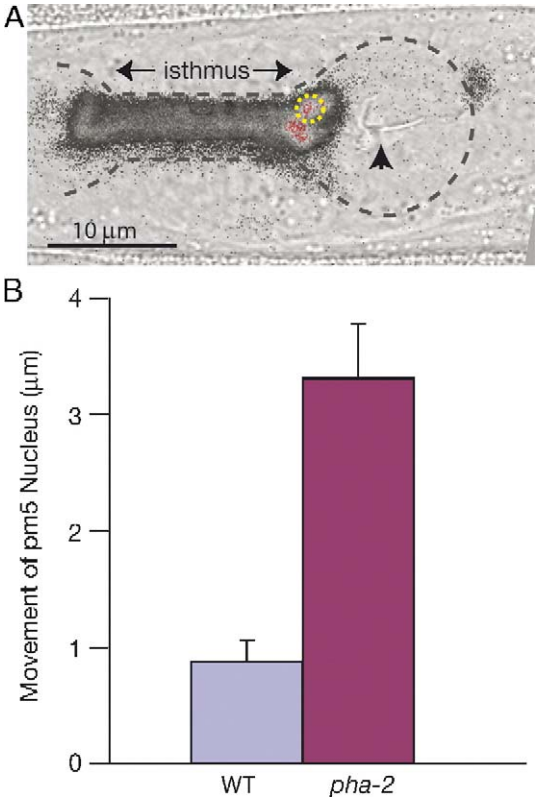

Fig. 7. Optical tweezers can move pm5 cell nuclei more readily in *pha-2* mutants. (A) Overlay of a bright field image and of digitalized GFP signal in a wild-type L1 larva transgenic for *pPHA-2*::*GFP-E*. The pharynx is outlined with a black dotted line. One pm5 nucleus is encircled with a yellow dotted line. Such a nucleus could be held with an optical trap while moving the specimen stage. Arrowhead indicates the position of the grinder within the posterior bulb. The pharyngeal isthmus is also indicated. (B) The "movement of pm5 nucleus" represents how much a nucleus could be moved before falling out of the optical trap and was expressed in μm. Note that pm5 nuclei of *pha-2* mutants could be moved much more than those of wild-type worms.

Ectopic expression of pha-2 induces ectopic expression of pACE-1:gfp and pACE-2::GFP

We wanted to explore the hypothesis that the *ace-1* and/or *ace-2* genes are transcriptional targets for PHA-2. To this end, we created a heat-shock-inducible construct with the full-length *pha-2* cDNA fused to the *hsp-16-2* promoter, then generated transgenic worms carrying this construct together with either the *pACE-1*::*GFP* or *pACE-2*::*GFP* constructs described earlier. Transgenic adult worms were allowed to lay eggs for 1 h at 20°C, and the eggs were heat shocked at 33°C for 1 h then allowed to develop at 15°C. All transgenic eggs exposed to 33°C arrested before the comma stage while nontransgenic heat-shocked embryos developed normally. Usually, *pACE-1*::*GFP* is first expressed at the 1-1/2-fold stage in only one or very few cells (Figs. 8A–B). Heat-shocked transgenic embryos expressed pACE-1::GFP in many more cells and also beginning at an earlier stage (Figs. 8E–F). Similar results were obtained with *pACE-2*::*GFP*, although the effect was not as pronounced due to its naturally higher and more ubiquitous expression (Figs. 8C–D and G–H). These results suggest that the *ace-1* and *ace-2* genes may be direct targets for PHA-2 regulation.

Transgenic embryos carrying the *hsp-16-2*:*pha-2cDNA* and the *pACE-4;ACE-3*::*GFP* constructs did not show heat-shock induction of GFP positive cells, indicating that the *ace-4;ace-3* operon is not regulated by *pha-2* (data not shown). However, all these transgenic embryos also arrested when heat shocked.

In the course of the present series of experiments, we noted that all transgenic embryos arrested their development soon after heat shock treatment. We therefore wished to determine if this was due to the ectopic/overexpression of *pha-2* or merely to the titration of important factors binding to the extrachromosomal arrays that carry multiple copies of the *hsp-16-2* promoter (which could possibly render the embryos less resistant to heat-shock). To distinguish between these possibilities, we generated two new types of transgenic animals: animals carrying only the plasmid pBK125 (*hsp-16-2*::*GFP*), and animals carrying only the *hsp-16-2*:*pha-2cDNA*::*GFP*. Embryos carrying the *hsp-16-2*::*GFP* or *hsp-16-2*:*pha-2cDNA*::*GFP* constructs showed heat shock induction of GFP in many cells (fully comparable to *hsp-*

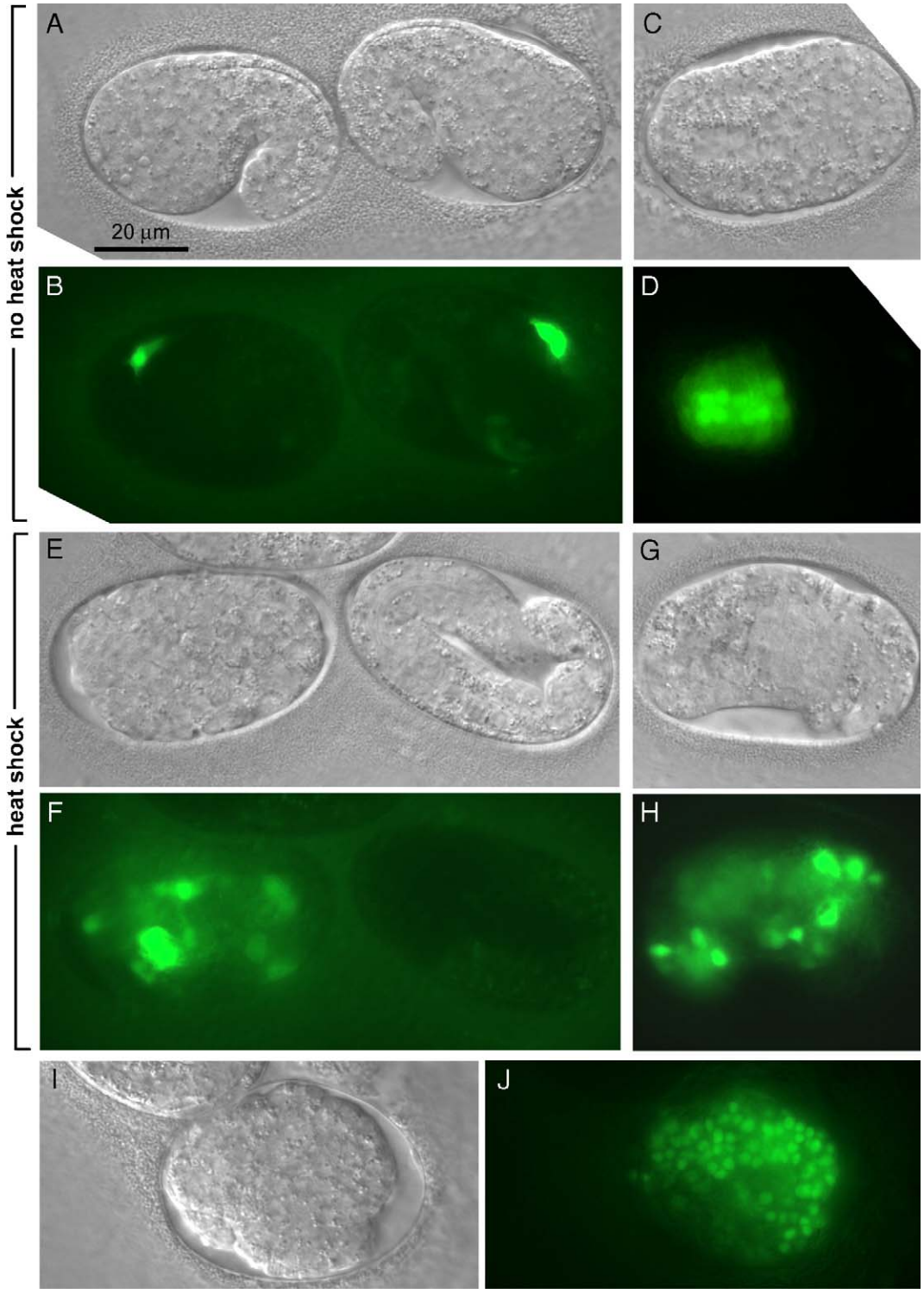

Fig. 8. Ectopic expression of *pha-2* induces expression of *pACE-1*: :*GFP and pACE-2*: :*GFP* reporters. Panels A, B, E and F show typical embryos transgenic for *pHSP*: :*PHA-2cDNA + pACE-1*: :*GFP.* Panels C, D, G and H show typical embryos transgenic for *pHSP*: :*PHA-2cDNA + pACE-2*: :*GFP.* (A and B) Without heat shock treatment *pACE-1*: :*GFP* is first expressed in very few cells at 1-1/2-fold stage. In panels C and D, the embryo expresses the *pACE-2*: :*GFP* construct in many cells by approximately 320 min of development. (E and F) After heat shock all transgenic embryos arrest at early stages and expresses *pACE-1*: :*GFP* in many cells. Note that the embryo to the right is non-transgenic and has developed normally to the 3-fold stage. (G and H) Heat-shocked embryo that has arrested and expresses *pACE-2*: :*GFP* ectopically in many cells. Note expression is spread all over the embryo. Panels I and J show heat-shocked arrested embryo transgenic for *pHSP*: :*PHA-2cDNA*: :*GFP.* Note the widespread ectopic expression of *pha-2* in many cells of the embryo. PHA-2 is normally only expressed in a few pharyngeal cells in early embryos (Mörck et al., 2004).

16-2:*pha-2cDNA* + *pACE1*: :*GFP* or *pACE2*: :*GFP*) but only the embryos with *hsp-16-2*:*pha-2cDNA*: :*GFP* arrested after heat shock (Figs. 8I–J). This result shows that it is ectopic/overexpression of *pha-2* that causes embryos to arrest at an early stage and not some non-specific effect due to the *hsp-16-2* promoter being present at a high copy number.

The isthmus is occasionally deformed in the anc-1 mutant, but not in ace-1;ace-2 double mutants

Since the *ace-1* and *ace-2* genes are not expressed in *pha-2* mutants, we decided to examine the pharynx in *ace-1*, *ace-2* single mutants and in *ace-1;ace-2* double mutants. The single mutants showed no defects considering movement or the pharynx morphology. The double mutants exhibited an uncoordinated phenotype but the pharynxes were not visibly abnormal at any stage (data not shown). Loss of *ace-1* and *ace-2* expression in the pm5 cells of *pha-2* mutants is therefore most likely not the only cause of the pharyngeal defects.

In *pha-2* mutants, the highly penetrant isthmus deformation (100% of animals) is always preceded by a mispositioning of the pm5 nuclei (Mörck et al., 2004). The *anc-1* (abnormal nuclear anchorage) mutant has also been reported to have misplaced cell nuclei (Hedgecock and Thomson, 1982). *anc-1* is homologous to the mammalian Syne proteins and is required for nuclear and mitochondrial attachment (Starr and Han, 2002). To visualize the pm5 nuclei, we introduced the *pPHA-2*: :*GFP-E* construct into *anc-1* and studied the pharynx in detail. In *anc-1* mutants, some nuclei of the isthmus pm5 muscle cells are occasionally displaced anteriorly (12% of worms; $n = 276$), a defect seen in 100% of *pha-2* worms. In the great majority of the *anc-1* mutant worms, the pharynx appears normal in shape (Figs. 9E–F). In very few worms (1.2%, $n = 254$), the pharynx was malformed in a fashion similar to that of *pha-2* mutants (Figs. 9C–D, G–H). We conclude that misplacement of pm5 nuclei in itself only rarely results in the severe pharyngeal phenotype seen in *pha-2* mutants.

To explore the hypothesis that the misplacement of pm5 nuclei in the *anc-1* mutant may be due to abnormal expression of the *ace* genes, we introduced the *pACE-1*: :*GFP* construct into *anc-1* mutants: expression of GFP in these transgenic did not differ from that produced in a wild-type background (data not shown). We also tested if the frequency of the *pha-2*-like phenotype could be increased by incubating *anc-1* mutant eggs on culture plates containing aldicarb, an acetylcholinesterase inhibitor. Wild-type and *anc-1* embryos were transferred to plates containing different concentrations of aldicarb (0.2 mM, 0.6 mM, 0.8 mM, 1.0 mM, 1.6 mM or 2.0 mM) and were allowed to develop, hatch and grow on the plates overnight. Worms grown on high concentration (0.8–2.0 mM) were totally

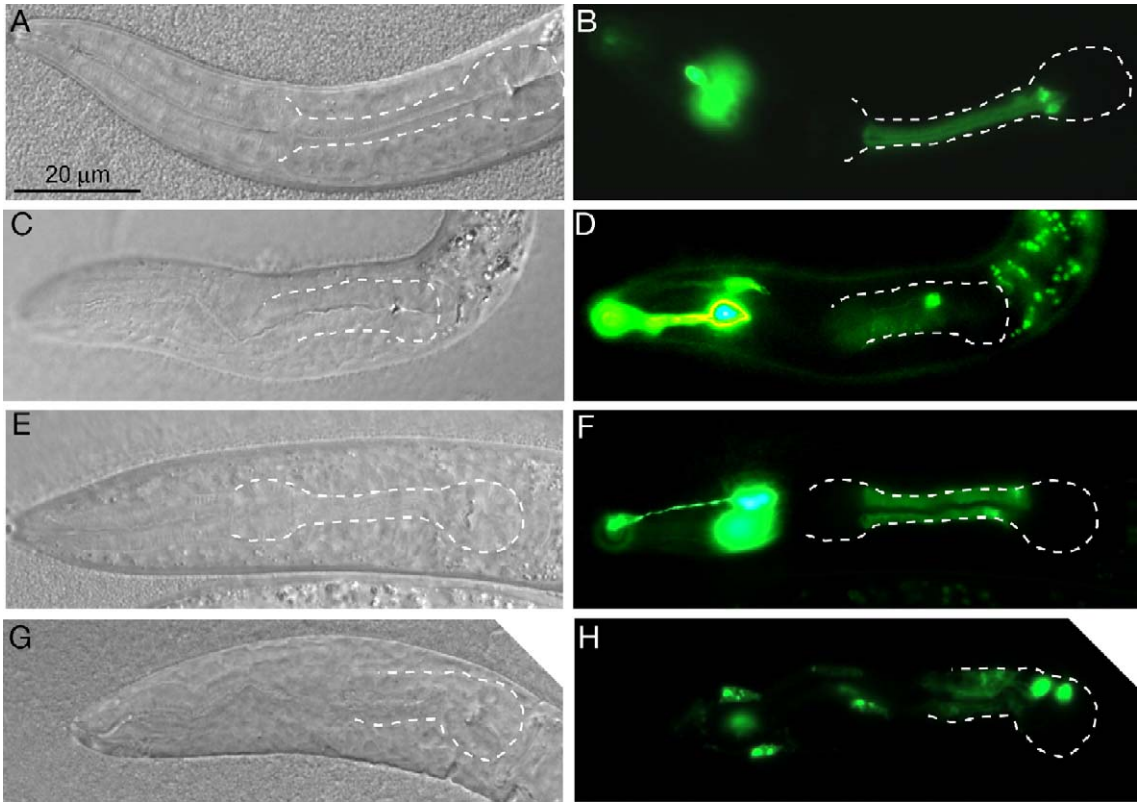

Fig. 9. *anc-1* mutants occasionally have pharyngeal defects similar to the *pha-2* phenotype. DIC and GFP images of L1 larvae transgenic for *pPHA-2*: :*GFP-E*. Panels A and B show a wild-type larva. Note that the pm5 cell nuclei are positioned at the posterior end of the cell, within the terminal bulb. Panels C and D show a *pha-2* mutant. The image in panel D is overexposed to show the faint GFP expression in the pm5 cells. As previously reported, the *pha-2* mutant expresses *pPHA-2*: :*GFP-E* only very weakly in the pm5 cells (Mörck et al., 2004). The GFP-positive cell nucleus in the posterior part of the isthmus corresponds to the I4 interneuron. Panels E and F show an *anc-1* mutant grown on plates with a normal pharynx. Note that the shape of the isthmus is normal although one of the pm5 cell nuclei is clearly misplaced anteriorly. Panels G and H show an *anc-1* mutant in which the pharynx is severely malformed and resembles that of the *pha-2* mutant in panel C.

paralyzed and did not pump their pharynxes. At these aldicarb concentrations, no abnormal pharynx morphology was detected either in wild-type worms or *anc-1* mutants. When grown on lower aldicarb concentrations, the worms had impaired movement but were able to pump their pharynxes and feed, albeit slowly. However, even at these concentrations, there was no significant increase in the frequency of the *pha-2*-like phenotype (data not shown). This indicates that the combination of *anc-1* mutation plus systemic/acute inhibition of acetylcholinesterases does not reproduce the *pha-2* situation. It is possible that the *anc-1* mutant is not an ideal model for these experiments or that aldicarb treatment is too acute and systemic to mimic properly the *pha-2* mutant.

Discussion

The main findings of the present study are (i) the *pha-2* (*ad472*) mutation specifically impairs the pharyngeal expression of *pha-2*; (ii) in the *pha-2* mutant, the cytoskeleton of the pm5 cells is measurably weaker than in normal cells and is severely disrupted by dilated tubular structures and organelles such as mitochondria; (iii) the pm5 cells of the *pha-2* mutant do not express the acetylcholinesterase genes *ace-1* and *ace-2*; (iv) ectopic expression of *pha-2* induces ectopic expression of the *ace-1* and *ace-2* genes; and (v) the *anc-1* mutant with mislocalized pm5 cell nuclei occasionally shows an isthmus phenotype similar to that of *pha-2* worms.

The *anc-1* mutant is the only known mutant besides *pha-2* that exhibits misplaced pm5 cell nuclei. However, in contrast to *pha-2* worms, the pharynx of *anc-1* mutants is generally normal in overall shape (Fig. 9) except in rare cases (1.2%) in which the isthmus deformed as in the *pha-2* mutant. The function of the ANC-1 protein is to anchor the nuclei to the actin cytoskeleton (Hedgecock and Thomson, 1982; Starr and Han, 2002). It therefore seems that misplacement of organelles is a contributing but generally insufficient cause for deformation of the isthmus.

Could the lack of *ace-1* and *ace-2* expression in the pm5 cells of the *pha-2* mutant contribute to the deformation of these cells in the mutant? Clearly, this cannot in itself be a sufficient cause for the phenotype since the *ace-1;ace-2* double mutant has no pharyngeal defects. Furthermore, some acetylcholinesterase activity is likely still present in these cells of the *pha-2* mutant since they express the *ace-4;ace-3* bicistroninc operon (Fig. 4). However, we have shown using optical tweezers that the pm5 nuclei of the *pha-2* L1 larvae are easily moved within the cells, indicating a weakened cytoskeleton in these cells. It is possible that the lack of *ace-1*/*ace-2* expression in combination with a weakened cytoskeleton is a contributing factor for the deformed isthmus phenotype because the pm5 cells may be unable to rest completely between contractions due to insufficient levels of acetylcholinesterase. We are tempted to propose the following scenario to explain the pharyngeal phenotype in the *pha-2* mutant: In this mutants, the pm5 nuclei are misplaced during the elongation of the pm5 isthmus cells at the 2-fold embryonic stage (Mörck et al., 2004), possibly due to some cytoskeletal defect, as suggested by our optical tweezer experiment. Later, when the pharynx starts pumping, the lack of *ace-1* and *ace-2* expression may exacerbate the cytoskeletal defects. This results in further disruption of the cytoskeleton over time accompanied by displacement of more organelles, increasing cell deformation with age and chronic contraction evidenced by the open, bacteria-filled isthmus lumen in the mutant. Note that other crucial changes accounting for the isthmus phenotype may take place within the pm5 cells: our model obviously reflects our still limited knowledge.

This model is consistent with the known roles of acetylcholinesterases. The function of AChE at neuromuscular junctions is to rapidly eliminate any excess of acetylcholine, and hence to reset synapses between stimulations. Experimental (in rats) or poison-related (patients with organophosphorous poisoning) inhibitions of AChE have been shown to result in muscle damages, including disruptions of the muscle fibers (John et al., 2003; Mense et al., 2003). This is most likely due to the harmful consequences of chronic muscle contractions caused by elevated or accumulating levels of acetylcholine that is not effectively eliminated in the absence of AChE. Indeed, AChE inhibition is known to lead to muscle degeneration accompanied by centralization of the muscle nuclei and the presence of degenerating profiles (Jeyarasasingam et al., 2000). Also, it is a long-standing observation that inhibition of AChEs leads to destruction of the muscle fibers accompanied by a breakdown of the sarcoplasmic reticulum (SR) (Salpeter et al., 1979).

When activated, acetylcholine receptors open up to allow an inward flow of sodium, potassium and calcium ions, and it is documented that excess of calcium overloads the SR (sarcoplasmic reticulum) and causes swelling (Kawabuchi, 1982). It has also been shown that calcium dependent proteases can attack Z-disks and cause muscle degeneration in response to excessive activation of the acetylcholine receptors (Kawabuchi, 1982; Salpeter et al., 1979). In *C. elegans*, the morphology of the isthmus muscle cells is not fully comparable with vertebrate striated muscle cells since pm5 cells are non-striated (single sarcomere), and the filaments are not arranged in Z-disks with SR surrounding the disks. Rather, in the isthmus the SR is situated among the filaments. In *pha-2* mutants, we did not observe a clear degeneration of the muscle fibers, but we saw that the fibers become separated and disrupted within an isthmus that becomes increasingly deformed with age, possibly in part because of increased dilation of the SR. Thus, it seems that some aspects of *pha-2* mutant phenotype is consistent with what one would expect from the loss of AChE expression by the pm5 cells. If that is the case, the *pha-2* mutant could become a useful model for myopathic disorders that have their roots in misexpression or inactivation of acetylcholinesterases, such as congenital myasthenic syndrome.

In vertebrates a single gene encodes AChE but in *C. elegans*, there are three classes of acetylcholinesterases encoded by the genes ace-*1*, *ace-2*, *ace-3* and *ace-4*. *ace-1* and *ace-2* are together responsible for 95% of the enzyme

activity (Combes et al., 2003). *ace-3* and *ace-4* are located on the same chromosome only 356 nt apart from each other (Combes et al., 2003) and are thought to be included in the same operon (Grauso et al., 1988). Only *ace-1* and *ace-2* show pm5 cell-specific expression within the pharynx (Combes et al., 2003; Culetto et al., 1999). Single mutants of the *ace* genes show no visible phenotype, but double-mutants of *ace-1* and *ace-2* exhibit a severe uncoordinated phenotype (Culotti et al., 1981; Johnson et al., 1981) and triple mutants of *ace-1*, *ace-2* and *ace-3* are lethal (Johnson et al., 1988). In *C. elegans feh-1* (*Fe65-homolog-1*) mutants, the expression of *ace-1* and *ace-2* are decreased in the pharynx but the levels of *ace-3* is slightly increased. In these mutants, the pharynx does not contract and the worms are unable to feed and, as a consequence of this, arrest in the first larval stage (Bimonte et al., 2004). Since *ace-1;ace-2* double mutants exhibit no pharyngeal phenotype, the reason for the *feh-1* feeding defects and larval arrest must be dependent on other factors.

In *pha-2* (*ad472*) worms, the expression of the *pACE-4; ACE-3*::*GFP* is unaffected, even in the pm5 cells of the isthmus, suggesting that the *ace-4;ace-3* bicistroninc operon is regulated normally in these worms. It is however not clear whether the *ace-4;ace-3* operon could support sufficient levels of acetylcholinesterase activity to allow the pm5 muscle cells to rest between stimulations. In particular, it has been proposed that the *ace-4* gene may not encode a functional acetylcholinesterase and may even be a pseudogene (Combes et al., 2003).

Does *pha-2* directly regulate the *ace-1* and *ace-2* genes? The answer to that question is not known but our results indicate that these genes are indeed likely targets for PHA-2 regulation since ectopic *pha-2* expression induced ectopic/overexpression of the *pACE-1*::*GFP* and *pACE-2*::*GFP* constructs. The *pha-2* gene is expressed in many cells of the pharynx besides the pm5 (e.g., the pm4 cells, I4 and some epithelial cells), while *ace-1* and *ace-2* are expressed only in the pm5 cells within the pharynx, it is therefore clear that *pha-2* can not be acting alone to activate *ace-1* and *ace-2*. *pha-2* may also regulate *ace-1* and *ace-2* expression outside the pharynx: both genes are expressed in a subset of extrapharyngeal neurons (see Figs. 4 and 8; Mörck et al., 2004). The regulation of pharyngeal *pha-2* expression also seems to be controlled in an unusual manner since the *pha-2* (*ad472*) mutation is located 6 nucleotides upstream of the start ATG and impairs only expression in these cells. It will be very interesting to determine whether this regulation occurs at the post-transcriptional level and by what mechanism.

Acknowledgments

We thank Adrian Wolstenholme for the *pglc-2*:*lacZ* reporter strain, Ekkehard Schulze for the EC668 strain and the *C. elegans* Genetics Center (funded by the NIH National Center for Resources), particularly Theresa Stiernagle, for providing *C. elegans* strains. We thank Bengt Johansson and his staff at the Anatomy and Cell Biology Dept., Sahlgrenska University Hospital, for help with electron microscopy. We acknowledge the Swegene Centre for Cellular Imaging at Gothenburg University for the use of imaging equipment and helpful support from the staff. Thanks to Marika Hellqvist-Greberg for some solutions and phalloidin. Thanks to Peter Carlsson for the helpful comments on the manuscript. This work was supported by the Swedish funding agencies Vetenskaprådet, Cancerfonden and Carl Trygger Stiftelse.

References

Albertson, D.G., Thomson, J.N., 1976. The pharynx of *Caenorhabditis elegans*. Philos. Trans. R. Soc. London, Ser. B Biol. Sci. 275, 299–325.

Avery, L., Horvitz, H.R., 1989. Pharyngeal pumping continues after laser killing of the pharyngeal nervous system of *C. elegans*. Neuron 3, 473–485.

Avery, L., Shtonda, B.S., 2003. Food transport in the *C. elegans* pharynx. J. Exp. Biol. 206, 2441–2457.

Bimonte, M., Gianni, D., Allegra, D., Russo, T., Zambrano, N., 2004. Mutation of the feh-1 gene, the *Caenorhabditis elegans* orthologue of mammalian Fe65, decreases the expression of two acetylcholinesterase genes. Eur. J. Neurosci. 20, 1483–1488.

Bogue, C.W., Ganea, G.R., Sturm, E., Ianucci, R., Jacobs, H.C., 2000. *Hex* expression suggests a role in the development and function of organs derived from foregut endoderm. Dev. Dyn. 219, 84–89.

Brenner, S., 1974. The genetics of *Caenorhabditis elegans*. Genetics 77, 71–94.

Combes, D., Fedon, Y., Toutant, D., Arpagaus, M., 2003. Multiple ace genes encoding acetylcholinesterases of *Caenorhabditis elegans* have distinct tissue expression. Eur. J. Neurosci. 18, 497–512.

Culetto, E., Combes, D., Fedon, Y., Roig, A., Toutant, J.-P., Arpagaus, M., 1999. Structure and promoter activity of the 5′ flanking region of *ace-1*, the gene encoding acetylcholinesterase of class A in *Caenorhabditis elegans*. J. Mol. Biol. 290, 951–966.

Culotti, J.G., Von Ehrenstein, G., Culotti, M.R., Russell, R.L., 1981. A second class of acetylcholinesterase-deficient mutants of the nematode *Caenorhabditis elegans*. Genetics 97, 281–305.

Fire, A., 1992. Histochemical techniques for locating *Escherichia coli* β-galactosidase activity in transgenic organisms. Genet. Anal.: Tech. Appl. 9, 151–158.

Goksör, M., Enger, J., Hanstorp, D., 2004. Optical manipulation in combination with multiphoton microscopy for single-cell studies. Appl. Opt. 43, 4831–4837.

Grauso, M., Culetto, E., Combes, D., Fedon, Y., Toutant, D., Arpagaus, M., 1988. Existence of four acetylcholinesterase genes in the nematode *Caenorhabditis elegans* and *Caenorhabditis briggsae*. FEBS Lett. 424, 279–284.

Haun, C., Alexander, J., Stainier, D., Okkema, P.G., 1998. Rescue of *Caenorhabditis elegans* pharyngeal development by a vertebrate heart specification gene. Proc. Natl. Acad. Sci. 95, 5072–5075.

Hedgecock, E.M., Thomson, J.N., 1982. A gene required for nuclear and mitochondrial attachment in the nematode. Cell 30, 321–330.

Jeyarasasingam, G., Yeluashvili, M., Quick, M., 2000. Nitric oxide is involved in acetylcholinesterase inhibitor-induced myopathy in rats. J. Pharmacol. Exp. Ther. 295, 314–320.

John, M., Oommen, A., Zachariah, A., 2003. Muscle injury in organophosphorous poinsoning and its role in the development of intermediate syndrome. Neurotoxicology 24, 43–53.

Johnson, C.D., Ducket, J.G., Culotti, J.G., Herman, R.K., Meneely, P.M., Russell, R.L., 1981. An acetylcholinesterase-deficient mutant of the nematode *Caenorhabditis elegans*. Genetics 95, 261–279.

Johnson, C.D., Rand, J.R., Herman, R.K., Stern, B.D., Russell, R.L., 1988. The acetylcholinesterase genes of *C. elegans*: identification of a third gene (ace-3) and mosaic analysis of a synthetic phenotype. Neuron 1, 165–173.

Karabinos, A., Schulze, E., Klisch, T., Wang, J., Weber, K., 2002. Expression profiles of the essential intermediate filament (IF) protein A2 and the IF protein C2 in the nematode *Caenorhabditis elegans*. Mech. Dev. 117, 311–314.

Kawabuchi, M., 1982. Neostigmine myopathy is a calcium ion-dependent myopathy initially affecting the motor end-plate. J. Neuropathol. Exp. Neurol. 3, 298–314.

Krause, M., 1995. Techniques for analyzing transcription and translation. In: Epstein, H.F., Shakes, D.C. (Eds.), *Caenorhabditis elegans*: Modern Biological Analysis of An Organism. Academic Press, New York, pp. 513–529.

Laughton, D.L., Lunt, G.G., Wolstenholme, A.J., 1997. Reporter gene constructs suggest that the *Caenorhabditis elegans* avermectin receptor β-subunit is expressed solely in the pharynx. J. Exp. Biol. 200, 1509–1514.

Martinez Barbera, J.P., 2000. The homeobox gene *hex* is required in definitive endodermal tissues for normal forebrain, liver and thyroid formation. Development 127, 2433–2445.

Mello, C., Fire, A., 1995. DNA transformation. Methods Cell Biol. 48, 451–482.

Mense, S., Simons, D.J., Hoheisel, U., Quenzer, B., 2003. Lesions of rat skeletal muscle after local block of acetycholinesterase and neuromuscular stimulation. J. Appl. Physiol. 94, 2494–2501.

Mörck, C., Rauthan, M., Wågberg, F., Pilon, M., 2004. *pha*-2 encodes the *C. elegans* ortholog of the homeodomain protein HEX and is required for the formation of the pharyngeal isthmus. Dev. Biol. 272, 403–418.

Salpeter, M.M., Kasprzak, H., Feng, H., Fertuck, H., 1979. Endplate after esterase inactivation in vivo: correlation between esterase concentration, functional response and fine structure. J. Neurocytol. 8, 95–115.

Simmons, R.M., Finer, J.T., Chu, S., Spudich, J.A., 1996. Quantitative measurements of force and displacement using an optical trap. Biophys. J. 70, 1813–1822.

Smithers, L.E., Jones, C.M., 2002. *Xhex*-expressing endodermal tissues are essential for anterior patterning in *Xenopus*. Mech. Dev. 119, 191–200.

Starr, D.A., Han, M., 2002. Role of ANC-1 in tethering nuclei to the actin cytoskeleton. Science 298, 406–409.

Sulston, J.E., Hodgkin, J.A., 1988. Methods. In: Wood, W.B. (Ed.), The Nematode *Caernorhabditis elegans*. In Cold Spring Harbor Laboratory Press, Cold Spring Harbor, NY, pp. 587–606.